ESS-PM4
4th Plenary Meeting of the European Spallation Source
October 16-19, 1995
Weinfelden, Switzerland

Suitability of Steels as ESS Mercury Target Container Materials

Y. Dai

Paul Scherrer Institut, 5232 Villigen PSI, Switzerland

ABSTRACT

A liquid mercury (Hg) target concept has been selected as the first priority development target for the European Spallation Source (ESS). The stability of the Hg target container is one of the most important issues, as under high intensity 1.35 GeV proton irradiation the beam window will be subject to very intensive radiation damage and high thermomechanical loads. In the present report, the material selection for the container will be considered, discussing mostly the data-base accumulated by the fusion program. Two candidate materials, solution annealed 316 type austenitic stainless steel (SA 316) and Sandvik HT-9 martensitic steel, are of primary interest.

1. Introduction

The target-group of the ESS has decided to study a liquid Hg target as the first priority target concept of the ESS target. One of the key issues of this target is the material of the container of the liquid Hg target, as the beam window will receive a very intense irradiation from both 1.35 GeV protons and spallation neutrons: the maximum proton beam density is about 100 $\mu A/cm^2$ for a 10 cm diameter beam of 5 MW [1], the corresponding displacement damage rate is about 0.15 displacement per atom (dpa) per day in steels, and the damage produced by neutrons is at a comparable rate [2], i.e. in total about 0.3 dpa per day. At the same time transmutation elements in particular helium and hydrogen but also other impurities will be produced at high rates. For example in iron about 300, 1450 and 330 appm/dpa of He, H and impurities, respectively, will be generated (calculated by using HETC code). Both radiation damage and transmutations will degrade the mechanical properties of the materials severely. In addition, the corrosion of mercury, which may be enhanced by irradiation, will shorten the lifetime of the container.

The beam window will be subject not only to an intensive radiation load but also to a high thermomechanical load which is due to: 1) the temperature gradient between inside and outside surfaces can be as high as about 90°C for a 2 mm thick wall [1], which produces a static thermal stress at a level about 50 to 100 MPa; 2) pulsed protons can generate stress from

Keywords: Mercury target, Structural materials, Radiation effects

pressure waves with an amplitude of several tens of MPa [3]; and 3) the deflection of the Hg flow at the window may produce ~50 MPa pressure. Therefore, the material of the liquid mercury target container (LMTC) should be able to support the mechanical loads, have a good radiation damage resistance and resist mercury corrosion.

At present, data on the property changes of materials under high energy proton irradiation is still very limited, especially for dose >1 dpa. However, a large database on materials for nuclear applications, particularly for future fusion reactors has been achieved in the last two decades by using fission neutron irradiation. These results can be a good reference, although there are large differences between high energy proton irradiation and fission neutron irradiation.

In the fusion program, both austenitic stainless steels and martensitic/ferritic (MF) steels are favoured as reference materials for the first wall and blanket of future fusion reactors. SA 316 is considered the most feasible one. The main disadvantage of austenitic stainless steels is the high void swelling rate at temperatures above ~400°C. The MF steels, on the other hand, present a ductile-brittle transition temperature (DBTT) which usually is increased substantially by irradiation [4]. In this paper, our interest will be focused on the behaviours of SA 316 and MF steel Sandvik HT-9 at low irradiation temperatures (≤~500°C, the optimised maximum design temperature of LMTC), as representative examples of both classes of steel, although SA 316 seems to be too soft to support the mechanical load on the beam window. Other possible classes materials for this application, such as vanadium and titanium alloys will not be discussed in this paper.

2. Microstructures and properties of unirradiated SA 316 and HT-9

2.1. Compositions and microstructure

Compositions of AISI 316 and HT-9 are given in Table 1 which includes also some other steels whose properties will be mentioned in the present paper.

In the solution annealed condition (~1050°C for ~2 h), SA 316 has a very low dislocation density, $< 10^{12}$ m^{-2}, and is precipitate free.

Table 1. Chemical compositions of steels discussed in the present paper (wt %)

Type	Steel	Fe	Ni	Cr	C	Mo	Mn	Nb	Ti	Si	Other
Austenitic	AISI 316	bal	13.7	17.3	0.05	2.26	1.64	-	-	0.56	
	AISI 304	bal	9.35	18.5	0.07	0.02	1.55	-	-	0.48	
	DIN 1.4970	bal	15.2	14.9	0.10	1.24	1.75	-	0.48	0.40	
	PCA	bal	16.6	14.3	0.05	1.95	1.83	-	0.31	0.52	0.05Al
Ferritic	HT-9	bal	0.50	12.0	0.02	1.00	0.50	-	-	0.40	0.5W, 0.33V
	9Cr-1MoVNb	bal	0.09	8.61	0.08	0.90	0.37	0.07	-	0.11	0.21V
	MANET-I	bal	0.92	10.8	0.14	0.77	0.7	0.16	-	0.37	0.2V
	EM10	bal	0.18	8.76	0.10	1.05	0.48	-	-	0.37	0.024N

Like other MF steels with 9-12Cr, HT-9 is usually used in a normalized (austenitizing for 5 min to 1 h at ~1040 - 1080°C, then quenching or air cooling) and tempered (at ~750 - 780°C for 1 to 2.5 h, then quenching or air cooling) condition. The heat-treatment produces a martensitic lath structure with carbide precipitates ($M_{23}C_6$ + MC) at grain boundaries and a partially recovered dislocation network [5,6].

2.2. Tensile properties

Unirradiated SA 316 is relatively soft. As indicated by the data in Table 2, the yield stress (YS) of SA 316 decreases continuously from about 300 MPa to about 160 MPa as temperature increases from room temperature to 430°C, although the ultimate tensile strength (UTS) remains ~ 500 MPa. However SA 316 has an excellent ductility. The uniform elongation is above 30%. Cold-working increases the yield stress of austenitic steels to high levels, however, at the expense of their ductility.

Compared to SA 316, HT-9 is stronger; both YS and UTS are much higher. With increasing temperature, the YS and UTS of HT-9 decrease slightly up to ~ 450°C, then very fast above 500°C. The uniform elongation (UE) and total elongation (TE) of HT-9 are, however, much lower than those of SA 316. The UE and TE of HT-9 first decrease with increasing temperature to a minimum at ~350°C, then increase with temperature.

Table 2 Tensile properties of SA 316 and HT-9 as a function of temperature

SA 316 [7]*					HT-9 [8]				
Temp. (°C)	YS (MPa)	UTS (MPa)	UE (%)	TE (%)	Temp. (°C)	YS (MPa)	UTS (MPa)	UE (%)	TE (%)
27	305	610	48	62	25	607	759	9.7	11.9
77	250	550	41	53	232	547	678	6.1	8.2
227	203	500	31	41	400	504	598	5.1	8.1
327	190	490	31	40	450	508	610	5.7	8.4
426	162	490	34	42	500	484	561	7.8	11.4
577	150	430	31	39	550	418	459	6.7	18.6

* Original data are of SA 316LN which should be not very different to those of SA 316.

2.3 Thermal stress resistance

Thermal stress resistance is an important parameter for the LMTC materials, as very high thermal stresses may be produced by pulsed high energy protons. The thermal stress resistance of materials is a function of thermal conductivity κ, thermal expansion coefficient α, Poisson's ratio ν, Young's Modulus μ and yield stress σ_y, and can be quantified by the relation [9]

$$M = \frac{2\sigma_y \kappa (1-\nu)}{\mu\alpha} \qquad (1)$$

HT-9 has a higher thermal conductivity than SA 316 (~24 W $m^{-1}K^{-1}$ to 16.2 W $m^{-1}K^{-1}$ at 100°C) and a lower thermal expansion coefficient (~11 μm $m^{-1}K^{-1}$ to 15.9 μm $m^{-1}K^{-1}$ at 100°C). These, together with the higher yield stress, result in a much superior thermal stress resistance for HT-9; the parameter M is 8.5 W m^{-1} for unirradiated HT-9 and 1.3 W m^{-1} for unirradiated SA 316 [9].

3. Radiation induced property changes

Data reviewed in this report are mostly from irradiations in both fast and mixed-spectrum reactors. The difference between these two types reactor irradiation is that in mixed-spectrum neutron irradiation, helium is produced in steels containing Ni by a two-step reaction with thermal neutrons:

$$^{58}Ni + n \rightarrow {}^{59}Ni + \gamma \quad \text{and} \quad {}^{59}Ni + n \rightarrow {}^{56}Ni + {}^{4}He \qquad (2)$$

In a fast reactor, with a lower thermal neutron flux, the helium production rate (< 1appm He/dpa in SA 316) is much lower than that in a mixed-spectrum neutron case (~10 -30 appm He/dpa) for Ni containing alloys.

Apart the neutron irradiation results, those of ion irradiation and implantation will also be reviewed.

3.1. SA 316

SA 316 is considered to be the most feasible structural material for the first wall and blanket of a fusion reactor because of the large database available from fission reactor applications and the extended manufacturing experience [4]. In addition to 316 type steels, a number of other Fe-Cr-Ni austenitic stainless steel compositions such as 304 type, PCA (Prime Candidate Alloy) and DIN 1.4970 (see Table 1 for the compositions) have been also investigated intensively in both SA and CW (cold worked) conditions. The results on these steels have been reviewed by a number of authors, e.g. [4,10-14] and will be sometimes shown as a comparison.

3.1.1. Microstructure and swelling

The irradiation induced microstructure in solution annealed austenitic stainless steels is strongly temperature dependent.

Limited data at low temperatures (< ~300°C) and low doses (≤0.5 dpa) shows that the main feature is the formation of small dislocation loops of interstitial type [15,16]. The average size of the loops is 1-2 nm and is almost independent of dose. The loop density was found to be as high as 2×10^{24} m^{-3} at 0.03 dpa for an irradiation performed at 90°C and to decrease by a factor ~10 after a 290°C irradiation [16]. The loop density was measured to be 2.9×10^{23} m^{-3} in the specimens irradiated to 0.5 dpa at 120°C [15], These data suggest that the density of loops saturates or even decreases at higher doses.

At 300°C and above, the small loops disappear. Instead, large (< 10 nm in diameter) Frank loops were observed [17,18]. Studies of both SA and CW 316 irradiated to 34 and 57 dpa in HFIR show that the Frank loop concentration increases slightly with temperature from 300 to 400°C, then decreases as the temperature increases to 500°C. The average size, however, increases continuously with temperature from ~10 nm at 300°C to ~21 nm at 500°C.

In SA 316 ,below 400°C, there are essentially no irradiation induced precipitates formed up to 20 dpa and very few small precipitates were observed at higher doses. At 400-500°C, M_6C and γ'-Ni_3Si phases were observed in HFIR irradiated specimens [19], and $M_{23}C_6$, M_6C, γ'-Ni_3Si, G and phosphides were observed in EBR-II irradiated specimens [19,20].

Small cavities were observed in SA 304L specimens at temperatures and doses as low as 120°C and 0.5 dpa (35 appm He) though in very low concentrations, $\sim 1.5 \times 10^{22}$ m^{-3} [15]. At 300-500°C, cavities are usually observed abundantly at high doses. With increasing temperature, the size of cavities increases and the density decreases [17,18].

Void swelling of austenitic stainless steels usually has a incubation period at lower doses, followed by a linear dose dependence (steady state swelling) with a rate up to 1% per dpa. The length of the incubation depends strongly on composition, heat treatment, temperature etc.. For SA 316, below 300°C, there is no or very low swelling [4,18,21]. At ~ 400°C, in the SA 316 irradiated at HFIR, swelling was still very low (< 1%) up to 57 dpa and 4300 appm He [18,21], but it can be also as high as 4% at ~ 35 dpa for other SA 316 steels [22]. This could be attributed to differences in the compositions.

3.1.2. Tensile properties and fracture toughness

At temperatures below 400°C the small dislocation loops and dislocation networks formed during irradiation result in a substantial increase of the yield strength. The yield strength is proportional to the square root of the dose at low doses and saturates at high doses. The saturation is dependent on the temperature but independent of the initial condition (annealed, cold worked or weld) of the steels and of the irradiation neutron source, when they are compared on the basis of dpa [10,12]. At 300°C the yield strength saturates at about 800 to 900 MPa at a dose of ~10 dpa. In the case of saturation, the yield stress reaches about the same level as the ultimate stress, i.e. σ_u/σ_y is equal to ~1 and no work hardening is present in the tensile curve.

The change in ductility due to irradiation at low temperatures is still uncertain due to the few data available, especially at around 100°C. Generally, in the temperature range from 200 to 400°C, at doses between 10 and 30 dpa, the UE of the steels decreases to less than 1%, followed by some recovery at higher doses. The UE is usually greater than 1% at a temperature between 400 and 600°C and greater than 5% at 50°C. Although the UE is very low at temperatures between 200 and 400°C, the TE is maintained above 5% for the steels irradiated up to 44 dpa / 3500 appm He in HFIR and other reactors [7,10,11, 23-26], see Fig. 1. This indicates that the steels still have a substantial capacity for plastic deformation.

Helium and hydrogen effects on tensile properties were also studied by post-implantation tests at 200°C in SA 316L base material and at 200 and 400°C in its welds, with helium and hydrogen concentration up to 375 and 2750 appm, respectively [27]. The results show that the effect of helium implantation is more pronounced than that of hydrogen implantation. At 200°C hardening and reduction of ductility occurred. At 400°C most hydrogen implantation induced changes are recovered. Ductile failure were observed in all cases.

The hardening and the loss of ductility result a significant decrease in the fracture toughness (resistance to crack initiation) and even more severely in the tearing modulus (resistance to crack propagation). For SA steels and their welds, the fracture toughness, K_{IC}, decreases from ~300 MPa $m^{1/2}$ at unirradiated condition to about 50 to 100 MPa $m^{1/2}$ at the saturation dose level (< ~10 dpa) and the tearing modulus decreases from ~300 to as low as 10 to 20 at the same time [28-30].

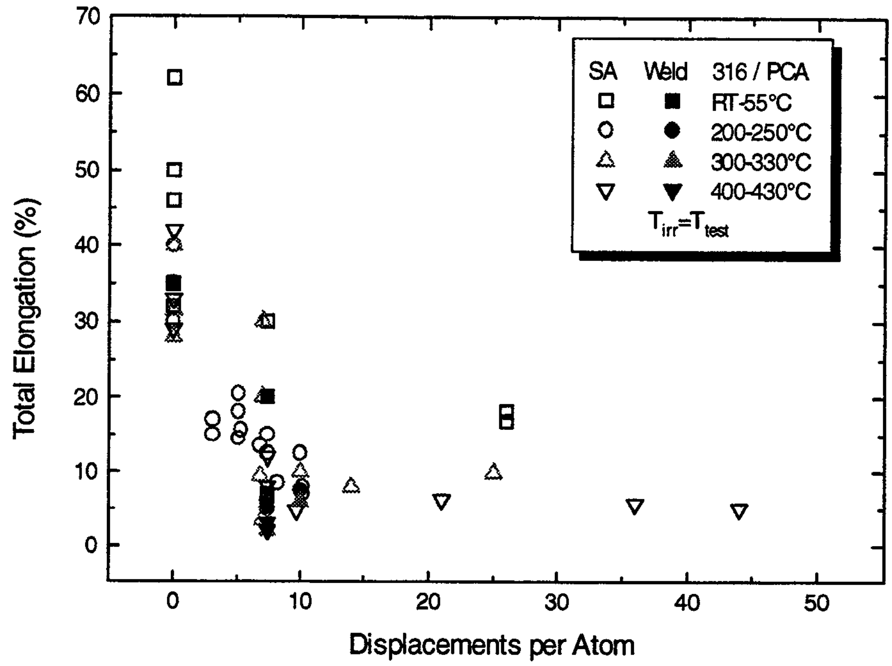

Fig. 1 Total elongation of SA 316 / PCA and their welds as a function of irradiation dose. Data are quoted from [7,10,11,23-26].

3.1.3. Creep and rupture

The effects of irradiation damage can produce very large changes in dimensions in austenitic steels and their welds by means of void swelling and irradiation creep.

As mentioned above, as the LMTC window will be subjected to a high mechanical load, irradiation creep is an important consideration.

Limited data published in 1970s on solution annealed 316 type steels showed that the creep rate of SA steels was similar to or even lower than that of CW (~20%) ones [31-33]. This is supported by recent results demonstrating that at 400°C, there is essentially no difference in the creep rates of 10, 20 and 30% cold worked titanium modified 316 (D9) stainless steels [34]. Fig. 2 shows the results from [32,33] given as stress-normalised creep strain versus irradiation dose. The difference between two data bands may arise from the different compositions of the steels as well as from the different dose rates in the two irradiation sources. Creep rate was found to have either a linear dependence on dose rate [4,35] or to be proportional to the square-root of dose rate [4,31,36].

The irradiation creep rate of the stainless steels has a weak dependence on temperature in the range 200 to 600°C [4,10,31] but it has been found to increase substantially at 600°C for 316 and PCA irradiated in the ORR spectral tailoring experiment [10,37].

Only one set of data [38] showed that the higher He/dpa ratio in ORR increased the creep rate of 25% CW PCA as compared to an irradiation in FFTF. The increase is expected to be due mostly to the lower displacement rate in ORR [4]. The very limited data at relatively low helium concentration (≤ 200 appm) is insufficient to understand at this point the effects of helium on irradiation creep.

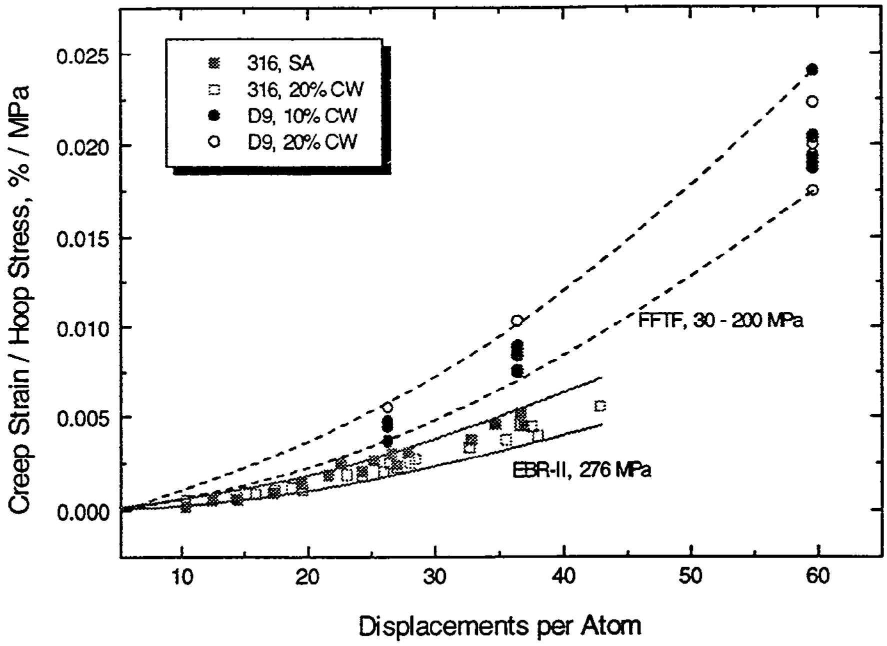

Fig. 2 Stress-normalised creep strains as a function of dose for 316 and D9 stainless steels (pressurized tubes) irradiated in EBR-II [32] and FFTF [34] at 400°C.

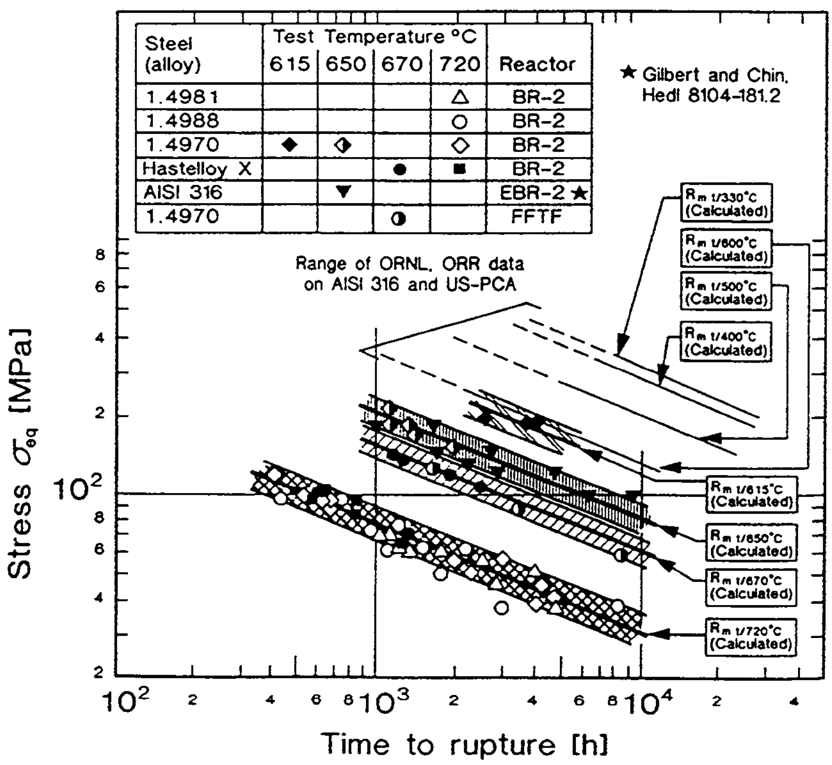

Fig. 3 Creep rupture life vs. stress of austenitic alloys irradiated in fast and mixed-spectrum reactors. (After [10])

At high temperatures (> 500°C), the loss of ductility and the reduction of creep rupture life are usually attributed to the growth and coalescence of helium bubbles on grain boundaries, namely helium embrittlement [10,39,40]. However, at 400°C and below there are no indications of helium embrittlement up to a concentration of 3500 appm [41].

Creep rupture life of a number of austenitic stainless steels was investigated in a temperature range from 575 to 720°C by performing in-pile experiments in reactors BR-2, EBR-II and FFTF [10,42,43]. The results of [43] are given in Fig. 3. The rupture lifetime obtained by [42] has a similar slope with stress but about half of value of that in Fig. 3. These results show that creep rupture life is affected by stress (at ~-5/2 power) and temperature, and is insensitive to factors such as the type of the austenitic alloy, heat treatments, the dose rate and the He to dpa ratio. The extrapolation of the results to low temperatures is demonstrated also in the figure.

3.1.4. Fatigue

Radiation and helium effects on fatigue life of austenitic steels [44-51] and their welds [52] have been investigated in a number of cases by performing post-irradiation or post-implantation tests, where the highest dose and helium concentration are 50 dpa and 4110 appm, respectively [48]. At 550°C and below, fatigue life shows no severe (less than a factor of 2) degradation in most cases [45-47, 49-51], although observations showed a reduction in fatigue life of CW steels by a factor of 3 to 10 at 430°C with low strain rate of 4×10^{-3} s^{-1} [45, 48]. The general trend is that the degradation decreases with decreasing temperature and increasing frequency or strain rate. Transition from large degradation and intergranular fracture at low cycle to no or little degradation and transgranular fracture at high cycles was observed [47,51].

3.2. Martensitic/ferritic (MF) steels

The high resistance to swelling and helium embrittlement of MF steels enables them to be widely used in nuclear applications and has made them the tentative candidate materials for the first wall and blanket in fusion reactors. A number of different type steels have been tested. Our interest is basically focused on HT-9 which is mainly used in the US. Some results on other MF steels with 9-12Cr, e.g. MANET (DIN 1.4914), 9Cr-1MoVNb and EM10 are also given below. The compositions of HT-9 and some other MF steels are given in Table 1.

3.2.1. Microstructures and swelling

Irradiation effects on the microstructure and swelling of MF steels are reported to be dependent on composition, irradiation temperature, irradiation source, dose, and also heat-treatment. The following general features are observed after irradiation at temperatures between 300 to 600°C:

- Irradiation produced dislocation loop density decreases with increasing temperature, but loop size remains constant. Above ~500°C, loops are unstable and the dislocation density remains constant or decreases with irradiation [8,53,54]
- Irradiation induced precipitation of G, α', M_6C and chi-phases were observed after irradiations at temperatures below ~550°C. The $M_{23}C_6$ phase showed no change during irradiation [6, 53-55].
- Helium bubbles were observed in the MF steels irradiated with mixed-spectrum neutrons at 300 to 600°C [56]. Voids, however, were mainly observed at 400 to 500°C [54,56,57]. Void swelling has maximum values in the range of 400 to 450°C [6,54-57].
- HT-9 shows an extremely high swelling resistance [6,54,55] with a swelling rate as low as 0.012%/dpa under fast neutron irradiation up to 208 dpa [58] and mixed-spectrum neutron irradiation up to 37 dpa and ~87 appm He [54] at 400°C.

3.2.2. Tensile properties

Irradiation induced hardening in MF steels is temperature dependent. The YS of HT-9 irradiated in FFTF rises sharply with decreasing temperature from about 420°C down to about 360°C (inlet temperature of FFTF). At 450°C and above, there was essentially no change or even a decrease in YS [4,59]. This phenomenon has been widely observed in MF steels [60,61]. The trend at low temperature seems to extend at least down to 300°C [62]. It is not clear how the strength evolves with irradiation temperature from 300°C down to 25°C as the increase of YS is similar at 300°C and 25°C at a similar dose. The hardening saturates at <10 dpa in HT-9 irradiated in HFIR and EBR-II [60,63] but at a much lower dose (about 1 dpa) in MANET I irradiated in HFR-Petten at 253°C [64].

The effects of irradiation on the ductility of MF steels is less pronounced than in the case of austenitic stainless steels, but the ductility of unirradiated MF steels is already much lower than that of austenitic stainless steels. In Fig. 4, data is also included for unirradiated steels after ageing (e.g. 5000 h at the irradiation temperature), showing essentially no difference with the unaged steels. From the limited data it can be seen that at 450 and 500°C the ductility is influenced little by irradiation. At 400°C and below the ductility decreases but the TE is generally above 3%, except for those irradiations at room temperature to 5-10 dpa, which show the largest reduction in ductility.

The data described above is for materials irradiated by neutrons. However, there are also some limited results from high energy proton irradiation. Following irradiation with 800 MeV protons in the Los Alamos Meson Physics Facility (LAMPF) to ~1.5 dpa at 400°C, HT-9 showed a slight hardening and no significant change in ductility [65]. However, for MANET-I irradiated with 590 MeV protons in the PIREX facility in Paul Scherrer Institut to 0.4 and 0.7 dpa at 170 and 420°C and tested at 20 and 350°C, the results show substantial hardening and reduction of ductility [66].

Helium effects on the tensile properties of MF steels were investigated in Ni-doped HT-9 and 9Cr-1MoVNb irradiated in HFIR at 50°C to doses 5 - 24 dpa [63]. It showed that both the increase itself and rate of increase of yield strength with fluence increased with helium concentration, i.e. largest in the highest helium containing 2%Ni-doped materials, followed by 1%Ni-doped materials and normal materials. Whether the change is due to helium effects is not yet clear because: 1) The yield strength of unirradiated Ni-doped HT-9 and 9Cr-1MoVNb increased with Ni content. This means that Ni itself modifies the mechanical properties; 2) The absolute values of the increase of yield strength are almost independent of the amount of helium; 3) At 400°C and above the difference disappears [62]; and 4) Helium effects were not observed in MANET-I up to 500 appm He [67] and DIN 1.4914 with 100 appm He [68], but observed in 9Cr-1MoVNb and 9Cr-2W [69].

A review of the results produced by European laboratories with accelerator based injected He [67], concluded that in the lower temperature region (≤ ~400°C), no He effects on the mechanical properties had been detected.

3.2.3. Impact properties and DBTT

The irradiation effects of most concern in MF steels are reduction of fracture toughness, tearing modulus and increase of DBTT after irradiation.

For HT-9 irradiated with doses up to 180 dpa, the fracture toughness is little influenced in general, and the reduction of tearing modulus depends on irradiation temperature T_{irr}, as shown in Fig. 5. When T_{irr} is in between 380 - 420°C, the tearing modulus reduces to 70 - 40. When $T_{irr} \geq 450$°C, there is no reduction [59,71,72]. Results of irradiation at 360°C (Fig. 5) and 250°C [73] show larger reduction of tearing modulus when tested at 200 - 250°C, dropping to zero at room temperature. However, for irradiations at 50°C [74] and 90°C [73], the situation becomes better, as the tearing modulus is above 25.

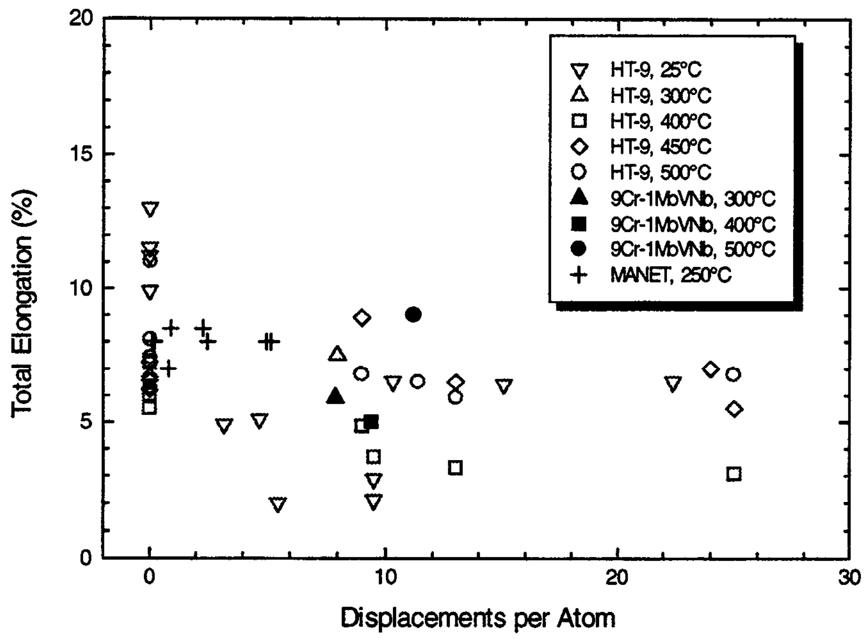

Fig. 4. Irradiation effects on the total elongation of HT-9, 9Cr-1MoVNb and MANET-I at different temperatures. Data are from [60,62-64,70]

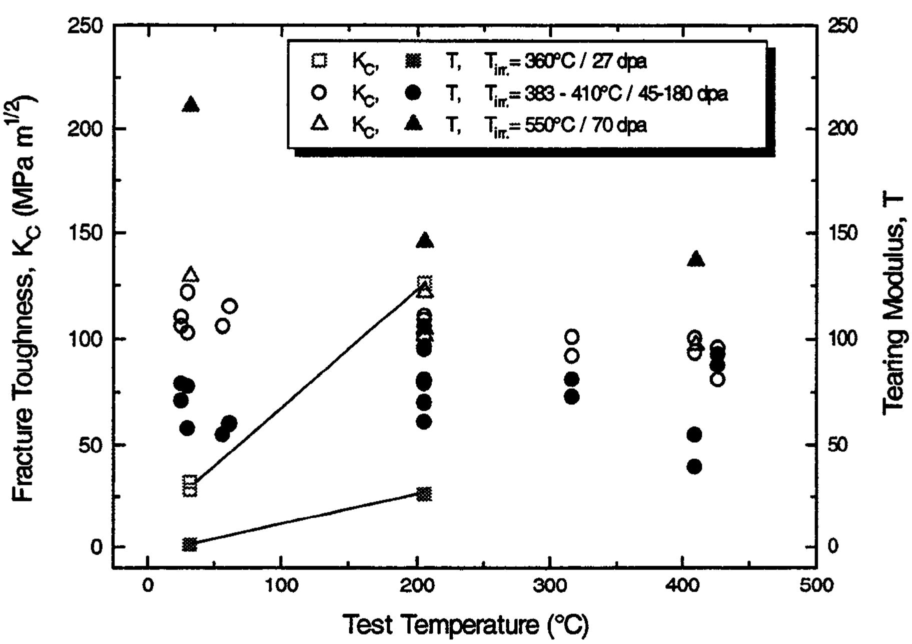

Fig. 5. Irradiation effects on fracture toughness and tearing modulus of HT-9. Data are from [59,71,72].

Increase of yield strength and loss of toughness in irradiated MF steels are accompanied by an increase (shift) of DBTT and a decrease of upper shelf energy (USE). The DBTT of unirradiated HT-9 is dependent somewhat on the heat treatment and specimen size, and varies normally between -10 to -60°C [75,76]. The shift of DBTT is found to be dependent on the irradiation temperature. As shown in Fig. 6, the shift of DBTT has a maximum at irradiation temperatures between ~150°-350°C; decreases rapidly between ~350° to 450°C and changes little above 450°C.

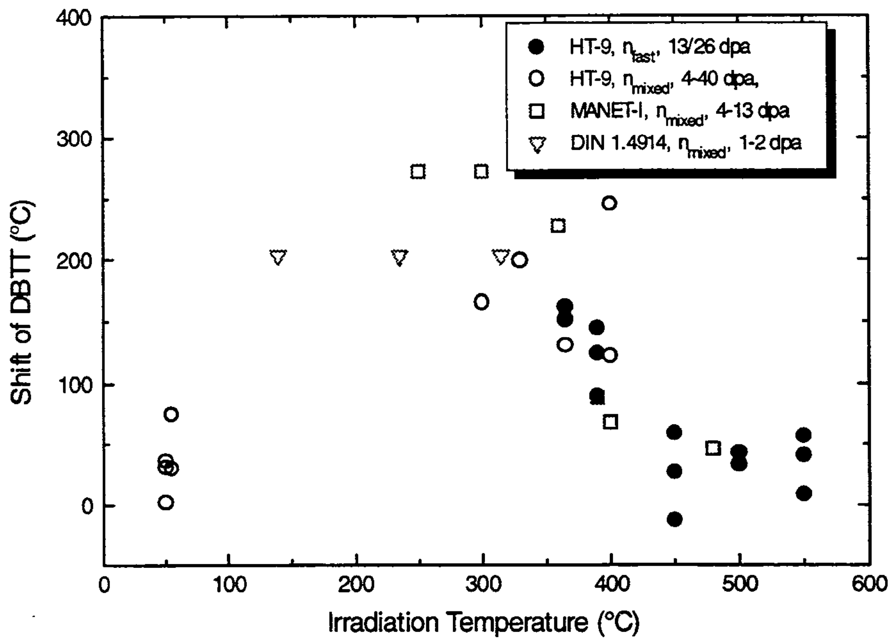

Fig. 6. Variation of DBTT with temperature for HT-9, MANET-I and DIN 1.4914 irradiated with fast neutrons (in FFTF and EBR-II) and mixed-spectrum neutrons (in HFIR, ORR and HFR). Data are from [75-81].

The change of DBTT depends also on the irradiation source. The increase in DBTT of HT-9 irradiated with fast neutrons saturates to ~140°C, but in mixed-spectrum neutron irradiation cases it goes up to 245°C [77]. The reason is suspected to be the higher helium content produced by mixed-spectrum neutrons. The situation is not clear, though, since at the same irradiation conditions, 9Cr-1MoVNb in which less helium has been produced, shows an even larger difference in the DBTT shifts.

3.2.4. Creep and fatigue

Irradiation creep of HT-9 has been investigated during fast neutron irradiation to a dose as high as 208 dpa at 400°C [82]. Fig. 7 shows the dose and stress dependencies of the stress-normalized creep strain rate at the midwall of HT-9 pressurized tubes. The stress enhanced swelling is ignored. The increase of normalized creep rate with stress indicates a non-linear stress dependence. Below 450°C thermal creep is less pronounced than irradiation creep. There are still no results on helium effects on low temperature irradiation creep.

Fatigue results on MF steels are limited to low cycle or low strain rate (the order of $10^{-3}s^{-1}$) cases. Two tests were conducted at room temperature on HT-9 irradiated in HFIR to 10 and 15 dpa with 34 and 53 appm He. The results show that the number of cycles to failure N_f is greater in one case (10 dpa / 34 appm He)) and 3 times lower in the other (15 dpa / 53 appm He) as compared to the unirradiated steel [83]. However, another two tests show greater N_f of 9Cr-1MoVNb with 2.5 and 3.3 dpa (2 and 4 appm He) than that of unirradiated material. For MANET a number of tests were performed at low doses (≤1.6 dpa) and with helium up to 400 appm using dual beam (30 MeV protons and 104 MeV α-particle) irradiation[84,85] and 590 MeV proton irradiation [66,86,87]. Both post-irradiation [66,84-86] and in-beam [85-87] tests were conducted. Stress softening (stress decreasing with cycle number) was observed in all unirradiated, post-irradiated and in-beam isothermal fatigue tests under a strain-control mode. In-beam results show a reduction of less than a factor of 2 in N_f in the temperature range 300-420°C, which is less than the reduction of N_f in post-irradiation cases, a factor of ~1.5 to 15. At 250°C and below, the N_f of in-beam tests decreases by a factor of more than 2 [87]. Helium effects on N_f have been investigated by performing dual-beam tests with He/dpa ratios of 10 and 170 appm/dpa and show no significant difference at 450°C [84]. Helium effects at low temperatures (<400°C) have not yet been studied.

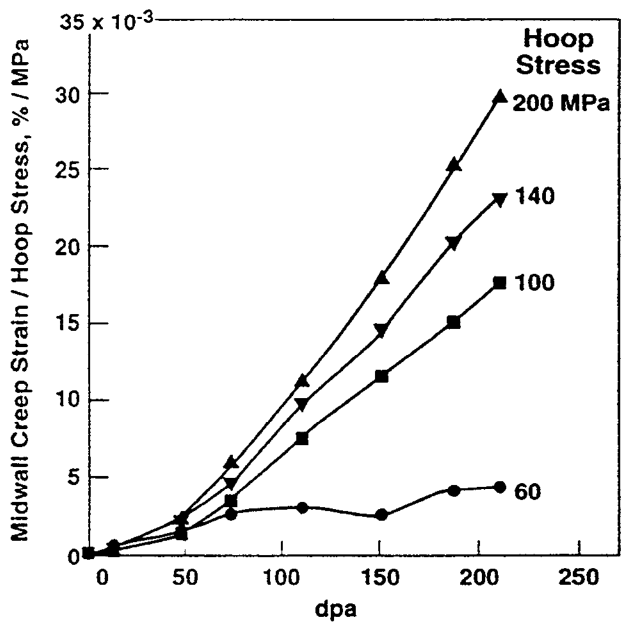

Fig. 7 Stress-normalized creep strains as a function dose for HT-9 (pressurized tubes) irradiated in FFTF at 400°C, after [82].

3.2.5. Hydrogen effects

Hydrogen embrittlement is a well known problem in MF steels. For example, it was found that fatigue lifetime of MANET-II (DIN 1.4914) was much shorter when tests were performed in hydrogen than in both vacuum and air at room temperature [88]. Another example is that charged hydrogen can significantly reduce ductility of both neutron irradiated and unirradiated 9Cr-2W martensitic steel at room temperature [89]. Hydrogen effects introduced by irradiation has been investigated in MANET-I after irradiation with 30 MeV protons between 80 and 500°C. 500 appm implanted H produced about 10 - 15% increase in yield strength and a slight reduction in ductility at 80 and 120°C showed but no effects at higher temperatures. The authors considered that the effects at 80 and 120°C might not be due to hydrogen but to 0.02 dpa damage produced during irradiation [90]. This view is reinforced by the second example above where it was found that hydrogen effects almost disappeared after 20 min of ageing at room temperature [89].

4. Liquid mercury corrosion

Liquid mercury corrosion of materials has been investigated in numerous cases [91-94]. Liquid Hg corrosion is the consequence of a slight solubility of materials in Hg, which depends on temperature. The variation of solubility of different chemical elements is given in detail in [95]. It shows that W, Ta, Mo, V, Fe, Si and C have good corrosion resistance, Be, Co, Cr, Ti and Zr have fair resistance, and Al, Cu, Mg, Mn, Nb, Ni, etc. have poor resistance to Hg corrosion [91,95].

The resistance of a given alloy is primarily a function of base metal resistance and amount of base metal present in the alloy. The influence of alloying additions depends on the resistance and quantity of each alloying element, and the nature of the alloying action, such as formation of new phases, solid solutions, intermetallics etc. For iron-base alloys, the corrosion was found to be dependent on total Ni, Cr and Mn content. Fig. 8 shows weight-losses of a number of iron-base alloys in slowly flowing Hg at 482°C (900°F) for 30 days [92]. It is clear that MF steels with generally less than 15% Ni+Cr+Mn additions have much better resistance than austenitic alloys with usually more than 30% of Ni+Cr+Mn additions. The typical Hg corrosion rate at 482°C for MF steels is less than 100 μm/yr and for austenitic alloys is about 500 to 1000 μm/yr [96].

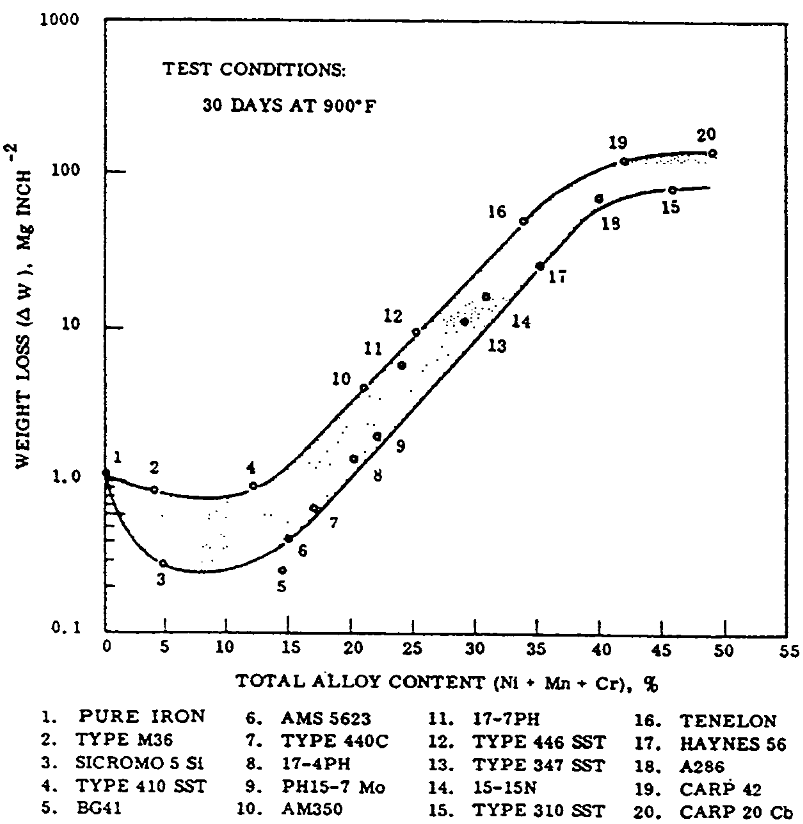

Fig. 8 Effect of Ni, Cr and Mn content on mercury corrosion of iron-base alloys, after [92].

The temperature dependence of mercury corrosion rate of materials can be expressed by an Arrhenius equation [92,95]:

$$\frac{d \ln \gamma}{dT} = \frac{E}{RT^2} \tag{3}$$

where γ is the corrosion rate, E is the activation energy in corrosion process, T is the absolute temperature, and R is the gas constant. For iron-base alloys, E is about 5400 cal/mole at low temperatures (<~700°F or 370°C) and about 38000 cal/mole at high temperatures [91]. At low temperatures, therefore, the corrosion rate is much less sensitive to temperature as compared to at high temperatures, where the corrosion rate changes by a factor 5 for a temperature change of about 100°C [92].

5. Discussion and conclusion

Comparing the above results from SA 316 and HT-9 at relatively low temperatures, it can be seen that HT-9 has certainly superior properties in terms of strength, thermal conductivity, thermal expansion, mercury corrosion resistance, void swelling and irradiation creep resistance. HT-9 has also less degradation in impact properties when the irradiation temperature is above 380°C. Although after irradiation the ductility of HT-9 is lower than that of SA 316, it is generally above 3% at doses up to 25 dpa and temperatures between 300 and 500°C (is not known between 25 and 300°C). Helium effects are not clear, particularly in the MF steels. Furthermore, the radiation effects on high cycle fatigue lifetime of HT-9 are not known. The main disadvantage of HT-9 is that the DBTT increases substantially in low temperature irradiations. In addition, it seems that hydrogen has greater effects in HT-9.

The stress level and operation temperature at the LMTC will determine which class steel will be applied. Based on above discussion and the maximum allowable design stress of HT-9 and annealed 316 [97,98], given as Fig. 9, it can be discussed in the following terms: For HT-9, the best application temperature range is from ~380 to 450°C where it has high strength and low degradation by irradiation. It should also be applicable in a wider temperature range from ~300 to 500°C. Outside this range, it may have severe embrittlement problem below 300°C and large thermal creep above 500°C. SA 316 is applicable up to ~350°C. At temperatures above 350°C, it may have large swelling. SA 316 is likely a better choice than HT-9 below 300°C when the stress is lower than its design stress level. Therefore application ranges of SA 316 and HT-9 can be given schematically as in Fig. 9. The upper margins added to original design stress levels are by considering that first, the design stress levels are much lower than the corresponding YS levels (see Table 2), especially for HT-9; and second, the materials will be rapidly hardened during the intensive irradiation. However, it is difficult to give definite values of the margins as radiation creep will be enhanced at higher stress levels.

It should be also noted that, as the existing results are limited, Fig. 9 is not a definitive conclusion. For example, two HT-9 windows have been irradiated in LAMPF to fluences about 3×10^{21} p/cm^2 (~9 dpa / 1700 appm He) at temperature <~180°C and show no visible degradation [99,100]. However, detailed examinations have yet to be carried out. Due to the same reason, the lifetime of the LMTC cannot be predicted at this point. A number of unknown issues and uncertainties which need to be investigated urgently are:

I). Helium effects on the overall mechanical properties are still not well understood. In steels, 1.35 GeV protons produce helium at a rate similar to that in iron, i.e. as high as

~300 appm He/dpa. This rate is much higher than in the fast neutron case, generally < 1 appm He/dpa, and in the mixed-spectrum neutron case, < 80 appm He/dpa, which depends strongly on both the Ni content of the steels and the precise neutron spectrum. For HT-9 which contains ~0.5% Ni, it is < 5 appm He/dpa in both types of neutron spectra. Therefore, if helium has an effect it will be more pronounced under high energy proton irradiations.

II). For HT-9, the shift of DBTT and the change of tensile and impact properties in the irradiation temperature range between 25 - 300°C are not known. Furthermore, the irradiation effects on fatigue lifetime are not clear either.

III). High energy protons can produce hydrogen at a very high rate, ~1400 appm H / dpa in iron for 1.35 GeV protons. In the case of HT-9, this may cause severe embrittlement, as has been shown by fatigue tests performed in hydrogen (see §3.2.5.). Since in post-irradiation tests most hydrogen may have escaped from the specimens, the results of post-irradiation tests may not reflect the real hydrogen effect.

IV). The mercury corrosion results reviewed in this paper are for the materials in a slow mercury flow. Corrosion may increase in a fast (several m/s) flow, especially at the beam window where the flow will be deflected. Irradiation may still enhance corrosion. These effects as well as stress corrosion cracking have not yet been investigated.

V). The details of the distribution of stress and temperature at the beam window and other parts of the container are under calculation.

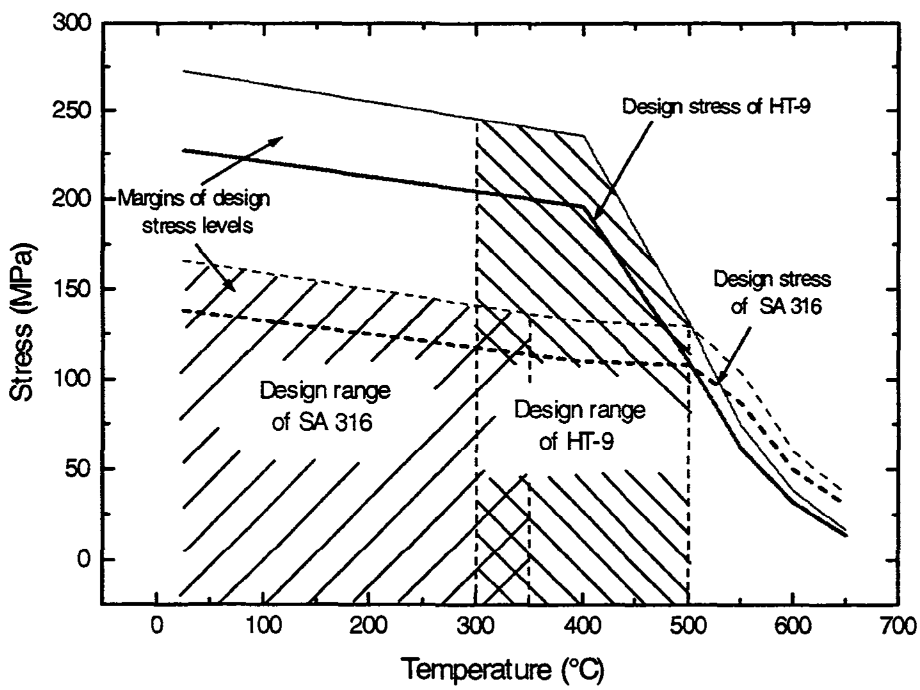

Fig. 9 Sketch showing design stress and temperature range for SA 316 and HT-9. The design stresses are quoted from design concepts of fusion reactor first wall and blanket structures [97,98].

Acknowledgements

The author is grateful to M. Victoria (PIREX-CRPP, PSI Villigen), W.F. Sommer (LAMPF, Los Alamos), H. Ullmaier (KFA, Jülich), F. Carsughi (KFA, Jülich) and G. Bauer (PSI Villigen) for their very useful discussion and careful reading the manuscript.

References:

[1] G. Bauer, **ESS 95-20-T**, 1995.
[2] H. Ullmaier and F. Carsughi, *Nucl. Instruments and Methods in Phys. Reseach*, **B 101** (1995) 406. or **ESS 95-17-T**, 1995.
[3] K. Skala and G. Bauer, this proceedings.
[4] F.A. Garner, in *Materials Science and Technology*, ed. R.W. Cahn, P. Haasen and E.J. Kramer, (VCH, Weinheim, 1994), vol. 10A, p. 419.
[5] J.M. Vitek and R.L. Klueh, in *Proc. Topical Conf. on Ferritic Alloys for Use in Nuclear Technologies*, (AIME, Warrendale, PA, 1984), p.551.
[6] P. Dubuisson, D. Gilbon and J.L. Séran, *J. Nucl. Mater.* **205** (1993) 178.
[7] M.G. Horsten and M.I. de Vries, *J. Nucl. Mater.* **212-215** (1994) 514.
[8] W.L. Bell, T. Lauritzen and S. Vaidyanathan, in *Proc. Topical Conf. on Ferritic Alloys for Use in Nuclear Technologies*, (AIME, Warrendale, PA, 1984), p. 113.
[9] S.N. Rosewasser, P.Miller, J.A. Dalessandro, J.M. Rawls, W.E. Toffolo and W. Chen, *J. Nucl. Mater.* **85&86** (1979) 177.
[10] M.L. Grossbeck, K. Ehrlich and C. Wassilew, *J. Nucl. Mater.* **174** (1990) 264.
[11] A. Kohyama, M.L. Grossbeck and G. Piatti, *J. Nucl. Mater.* **191-194** (1992) 37.
[12] G.R. Odette and G.E. Lucas, *J. Nucl. Mater.* **179-181** (1991) 572.
[13] G.R. Odette and G.E. Lucas, *J. Nucl. Mater.* **191-194** (1992) 50.
[14] J.C. Van Duysen, P. Todeschini and G. Zacharie, in *Effects of Radiation on Materials: 16th Inter. Sym.* (ASTM STP 1175, 1993), p. 747.
[15] S.J. Zinkle and R.L. Sindelar, *J. Nucl. Mater.* **155-157** (1988) 1196.
[16] N. Yoshida, *J. Nucl. Mater.* **174** (1990) 220.
[17] P.J. Maziasz, *J. Nucl. Mater.* **205** (1993) 118.
[18] S. Hamada, M. Suzuki, P.J. Maziasz, A. Hishinuma and M.P. Tanaka, in *Effects of Radiation on Materials: 14th Inter. Sym.* (ASTM STP 1046, 1989), p. 172.
[19] D.F. Pedraza and P.J. Maziasz, in *Radiation-Induced Changes in Microstructure: 13th Inter. Sym.*, (ASTM STP 955, 1987), p. 161.
[20] W.J.S. Yang, in *Radiation-Induced Changes in Microstructure: 13th Inter. Sym.*, (ASTM STP 955, 1987), p. 628.
[21] P.J. Maziasz, *J. Nucl. Mater.* **200** (1993) 90.
[22] J.L. Boutard, *J. Nucl. Mater.* **179-181** (1991) 1179.
[23] S. Jitsukawa, M.L. Grossbeck and A. Hishinuma, *J. Nucl. Mater.* **191-194** (1992) 790.
[24] J.D. Elen and P. Fenici, *J. Nucl. Mater.* **191-194** (1992) 766.
[25] F.W. Wiffen and P.J. Maziasz, *J. Nucl. Mater.* **103&104** (1981)
[26] S. Jitsukawa, P.J Maziasz, T. Ishiyama, L.T. Gibson and A. Hishinuma, *J. Nucl. Mater.* **191-194** (1992) 771.
[27] H. Schroeder and W. Liu, *J. Nucl. Mater.*, **191-194** (1992) 776.
[28] J.E. Pawel, D.J. Alexander, M.L. Grossbeck, A.W. Longest, A.F. Rowcliffe, G.E. Lucas, S. Jitsukawa, A. Hishinuma and K.Shiba, *J. Nucl. Mater.* **212-215** (1994) 442.
[29] G.E. Lucas and D.S. Gelles, *J. Nucl. Mater.* **155-157** (1988) 164.
[30] G.E. Lucas, *J. Nucl. Mater.* **206** (1993) 287.

[31] D. Mosedale, D.R. Harries, J.A. Hudson, G.W. Lewthwaite and R.J. McElroy, in *Proc. of Inter. Conf. on Radiation Effects in Breeder Reactor Structural Materials*, (AIME, New York, 1977), p.209.
[32] L.C. Walters, G.L. McVay and G.D. Hudman, in: *Proc. of Inter. Conf. on Radiation Effects in Breeder Reactor Structural Materials*, (AIME, New York, 1977), p.277.
[33] J.L. Straalsund, in: *Proc. of Inter. Conf. on Radiation Effects in Breeder Reactor Structural Materials*, (AIME, New York, 1977), p.191.
[34] F.A. Garner, M.L. Hamilton, C.R. Eiholzer, M.B. Toloczko and A.S. Kumar, in *Effects of Radiation on Materials: 16th Inter. Sym.*, (ASTM STP 1175, 1993), p. 696.
[35] A.S. Kruglov, M.E. Bul'Kanov, V.N. Bykov and Y.M. Pevchikh, *Atomnaya Energiya*, **48** (1980) 258.
[36] G.W. Lewthwaite and D. Mosedale, *J. Nucl. Mater.* **90** (1980) 205.
[37] M.L. Grossbeck, L.K. Mansur and M.P. Tanaka, in *Effects of Radiation on Materials: 14th Inter. Sym.*, (ASTM STP 1046, 1990), p. 537.
[38] M.L. Grossbeck and J.A. Horak, *J. Nucl. Mater.* **155-157** (1988) 1001.
[39] H. Ullmaier, *Nuclear Fusion*, **24** (1984) 1039.
[40] H. Schroeder, *J. Nucl. Mater.* **155-157** (1988) 1032.
[41] L.K. Mansur and M.L. Grossbeck, *J. Nucl. Mater.* **155-157** (1988) 130.
[42] R.J. Puigh and M.L. Hamilton, in *Effects of Radiation on Materials: 13th Inter. Sym.*, (ASTM STP 956, 1987), p. 22.
[43] C. Wassilew, K. Ehrlich and H.J. Bergmann, in *Effects of Radiation on Materials: 13th Inter. Sym.*, (ASTM STP 956, 1987), p. 30.
[44] M.L. Grossbeck and K.C. Liu, *Nuclear Technology*, **58** (1981) 538.
[45] M.L. Grossbeck and K.C. Liu, *J. Nucl. Mater.* **103&104** (1981) 853.
[46] K. Sonnenberg and H. Ullmaier, *J. Nucl. Mater.* **103&104** (1981) 859.
[47] I.S. Batra, H. Ullmaier and K. Sonnenberg, *J. Nucl. Mater.* **116** (1983) 136.
[48] M.P. Tanaka, S. Hamada, A. Hishinuma and M.L. Grossbeck, K. Sonnenberg, *J. Nucl. Mater.* **155-157** (1988) 957.
[49] W. Vandermeulen, W. Hendrix, V. Massaut and J. Van de Velde, *J. Nucl. Mater.* **155-157** (1988) 953.
[50] B. Van der Schaaf, *J. Nucl. Mater.* **155-157** (1988) 156.
[51] M.I. de Vries, in *Effects of Radiation on Materials: 11th Inter. Sym.*, (ASTM STP 782, 1982), p 665.
[52] A.A. Tavassoli, in *Effects of Radiation on Materials: 15th Inter. Sym.*, (ASTM STP 1125, 1992), p. 1103.
[53] R.L. Klueh, K. Ehrlich and F. Abe, *J. Nucl. Mater.* **191-194** (1992) 116.
[54] E.A. Little and L.P. Stoter, in *Effects of Radiation on Materials: 11th Inter. Sym.*, (ASTM STP 782, 1982), p. 207.
[55] P.J. Maziasz, R.L. Klueh and J.M. Vitek, *J. Nucl. Mater.* **141-143** (1986) 929.
[56] D.S. Gelles and L.E. Thomas, in *Proc. Topical Conf. on Ferritic Alloys for Use in Nuclear Technologies*, (AIME, Warrendale, PA, 1984), p.559.
[57] D. Gilbon, J.L. Séran, R. Cauvin, A. Fissolo, A. Alamo, F. le Naour and V. Lévy, in *Effects of Radiation on Materials: 14th Inter. Sym.*, (ASTM STP 1046, 1989), p. 5.
[58] C.Y. Hsu, D.S. Gelles and T.A. Lechtenberg, in *Radiation-Induced Changes in Microstructure: 13th Inter. Sym.*, (ASTM STP 955, 1987), p. 545.
[59] F.H. Huang, in *Effects of Radiation on Materials: 15th Inter. Sym.*, (ASTM STP 1125, 1992), p. 1267.
[60] R.L. Klueh and J.M. Vitek, *J. Nucl. Mater.* **182** (1991) 230.
[61] J.L. Séran, A. Alamo, A. Maillard, H. Touron, J.C. Brachet, P. Dubuisson and O. Rabouille, *J. Nucl. Mater.* **212-215** (1994) 588.

[62] R.L. Klueh and J.M. Vitek, *J. Nucl. Mater.* **150** (1987) 272.
[63] R.L. Klueh and J.M. Vitek, *J. Nucl. Mater.* **161** (1989) 13.
[64] B. van der Schaaf and M.I. de Vries, *Proc. IEA Workshop on Ferritic-Martensitic Steels*, (Tokyo, 1992), p. 259.
[65] R.D. Brown, M.S. Wechsler and C. Tschalär, in *Effects of Radiation on Material Properties: 13th Inter. Sym.*, (ASTM STP 956, 1987), p. 131.
[66] P. Marmy and M. Victoria, *J. Nucl. Mater.* **191-194** (1992) 862.
[67] M. Victoria, in *Proc. IEA Workshop on Ferritic-Martensitic Steels*, (Tokyo, 1992), p. 366.
[68] H. Schroeder, *Report KFA Jülich*, (Jül-2454, 1994).
[69] A. Hasegawa, N. Yamamoto and H. Shiraishi, *J. Nucl. Mater.* **202** (1993) 266.
[70] R.L. Klueh, J.M. Vitek na M.L. Grossbeck, *J. Nucl. Mater.* **104** (1981) 887.
[71] F.H. Huang and M.L. Hamilton, *J. Nucl. Mater.* **187** (1992) 278.
[72] F.H. Huang, *Engineering Fracture Mechanics*, **43** (1992) 733.
[73] D.J. Alexander, J.E. Pawel, M.L. Grossbeck and A.F. Rowcliffe, *Fusion Materials Semiannual Progress Report*, (DOE/ER-0313/16, ORNL, 1994), p. 173.
[74] F.H. Huang, in *Effects of Radiation on Materials: 14th Inter. Sym.*, (ASTM STP 1046, 1990), p. 459.
[75] R.L. Klueh and D.J. Alexander, in *Effects of Radiation on Materials: 16th Inter. Sym.*, (ASTM STP 1175, 1993), p. 591.
[76] R.L. Klueh and D.J. Alexander, in *Effects of Radiation on Materials: 16th Inter. Sym.*, (ASTM STP 1125, 1992), p. 1256.
[77] C. Wassilew, M. Rieth and B. Dafferner, in *Proc. IEA Workshop on Ferritic-Martensitic Steels*, (Tokyo, 1992), p. 295.
[78] R.L. Klueh, J.M. Vitek, W.R. Corwin and D.J. Alexander, *J. Nucl. Mater.* **155-157** (1988) 973.
[79] W.L. Hu and D.S. Gelles, in *Influence of Radiation on Material Properties: 13th Inter. Sym.*, (ASTM STP 965, 1987), p. 83.
[80] W.L. Hu and D.S. Gelles, in *Effects of Radiation on Materials: 14th Inter. Sym.*, (ASTM STP 1046, 1990), p. 453.
[81] R.L. Klueh and D.J. Alexander, *J. Nucl. Mater.* **212-215** (1994) 736.
[82] M.B. Toloczko, F.A. Garner and C.E. Eiholzer, *J. Nucl. Mater.* **212-215** (1994) 604.
[83] M.L. Grossbeck, L.M. Vitek and K.C. Liu, *J. Nucl. Mater.* **141-143** (1986) 966.
[84] R. Lindau and A. Möslang, *J. Nucl. Mater.* **178-181** (1991) 753.
[85] R. Lindau and A. Möslang, *J. Nucl. Mater.* **212-215** (1994) 599.
[86] P. Marmy, *J. Nucl. Mater.* **212-215** (1994) 594.
[87] P. Marmy, *Plasma Device and Operations,* (1995) in print.
[88] J.I. Shakib, H. Ullmaier, E.A. Little, R.G. Faulkner, W. Schmitz and T.E. Chung, *J. Nucl. Mater.* **212-215** (1994) 579.
[89] A. Kimura, H. Kayano and M. Narui, *J. Nucl. Mater.* **179-181** (1991) 737.
[90] K.K. Bae, K. Ehrlich and A. Möslang, *J. Nucl. Mater.* **191-194** (1992) 905.
[91] J.F. Nejedlik and E.J. Vargo, *Electrochem. Techn.*, **3** (1965) 250.
[92] J.F. Nejedlik and E.J. Vargo, *Corrosion*, **20** (1964) 384.
[93] A.H. Fleitman, A.J. Romano and C.J. Klamut, *J. Electrochem. Soc.*, **110** (1963) 964.
[94] A.H. Fleitman and J.R. Weeks, Nucl. Eng. and Design, 16 (1971) 266.
[95] *Metals in Mercury*, eds. C. Hirayama, Z. Galus and C. Guminski, (Pergamon Press, Oxford, 1986).
[96] Handbook of Stainless Steels, ed. D. Peckner and I. M. Bernstein, (New York, McGraw-Hill, 1977)

[97] S.N. Rosenwasser, P. Miller, J.A. Dalessandro, J.M. Rawls, W.E. Toffolo and W. Chen, in *Proc. Topical Conf. on Ferritic Alloys for Use in Nuclear Technologies*, (AIME, Warrendale, PA, 1984), p. 177.
[98] J. D. Gordon, J.K. Ganer, N.M. Choniem and J.F. Parmer, in *Proc. Topical Conf. on Ferritic Alloys for Use in Nuclear Technologies*, (AIME, Warrendale, PA, 1984), p. 157.
[99] M. Dubs and J. Ulrich, ICANS-XI, (Japan, 1990).
[100] W.F. Sommer, private communication.